Solar Water Splitting

DOI: 10.1002/anie.201004801

Water Splitting by Tungsten Oxide Prepared by Atomic Layer Deposition and Decorated with an Oxygen-Evolving Catalyst**

Rui Liu, Yongjing Lin, Lien-Yang Chou, Stafford W. Sheehan, Wangshu He, Fan Zhang, Harvey J. M. Hou, and Dunwei Wang**

When sunlight is used as direct energy input, water can be split into hydrogen and oxygen at conversion efficiencies similar to those of solar cells.[1] This process offers a method for energy storage to address the problem that the sun does not shine continuously, and is a particularly appealing approach to solar-energy harvesting.[2–4] Notwithstanding the intense research efforts, progress in this area is extremely slow. Efficient and inexpensive water splitting remains elusive. A key reason for the sluggish progress is the lack of suitable materials.[5] The "ideal" material must absorb strongly in the visible range, be efficient in separating charges using the absorbed photons, and be effective in collecting and transporting charges for the chemical processes. Such a material has yet to be found.[6]

The difficulties in finding a suitable material stem from the competing nature of intrinsic material properties (e.g., optical depth, charge diffusion distance, and width of the depletion region, among others), which leaves limited opportunity for tunability.[7] We recently demonstrated that heteronanostructures, a type of nanoscale material consisting of multiple components that complement each other, have a combination of properties which are not available in single-component materials.[8,9] For instance, we can add charge-transport components to oxide semiconductors to solve the issue of low conductivity that oxide semiconductors generally suffer.[8] In a similar fashion, one can add an effective catalyst to address the challenge that oxygen evolution is complex and tends to be the rate-limiting step.[10–12] These new materials will likely lead to significant improvement in solar water-splitting efficiencies. The success of a heteronanostructure design relies on the ability to produce high-quality components with interfaces of low defect density, and on the availability of various components. Here we show that crystalline WO_3 can be synthesized by the atomic layer deposition (ALD) method in the true ALD regime. When coated with a novel Mn-based catalyst, the resulting WO_3 survives soaking in H_2O at pH 7 and produces oxygen by splitting H_2O under illumination.

We choose ALD to prepare WO_3 because of the following advantages: 1) a high degree of control over the resulting materials; 2) excellent step coverage to yield conformal coatings; and 3) process versatility to tailor the composition of the deposit. WO_3 was studied because it is one of the most researched compounds for water splitting. The widely available literature makes it easy to compare our results with existing reports[13–15] and thus allows us to test the power of the heteronanostructure design. To avoid the production of corrosive byproducts during the ALD process[16] and to ensure the reaction occurs in the true ALD regime, we used $(t\mathrm{BuN})_2(\mathrm{Me_2N})_2\mathrm{W}$ as tungsten precursor and H_2O as oxygen precursor, as described in the Experimental Section (see Supporting Information for more details). Our first goal was to verify that the growth indeed takes place in the ALD regime. The dependence of the growth rate on the precursor pulse times and on the substrate temperature unambiguously confirms this. In addition, the excellent linear dependence of the deposition thickness on the number of precursor pulses supports the ALD growth mechanism and shows the extent of control we can achieve (see Supporting Information). That a long H_2O pulse time is necessary to initiate growth is a key finding of this work. Despite intentional strengthening of the oxidative conditions, as-grown WO_3 exhibited a tinted color, indicating the existence of oxygen deficiencies,[17] which was then corrected by an annealing step in O_2 at 550 °C. The crystalline nature of the product is manifested in the high-resolution (HR) TEM image in Figure 1a. We also synthesized WO_3 on two-dimensional $TiSi_2$ nanonets.[18,19] The uniformity and good coverage around the nanonet branches show that this deposition technique is suitable for the creation of heteronanostructures.

Ready dissolution of WO_3 in aqueous solutions with pH $\geq$ 4 is a significant challenge that impedes its widespread use.[20] We sought to solve this problem by coating WO_3 with an Mn-based catalyst. Derived from the Brudvig–Crabtree catalyst, this coating was prepared by thermally decomposing $[(H_2O)(\mathrm{terpy})\mathrm{Mn(O)_2Mn}(H_2O)(\mathrm{terpy})](NO_3)_3$ (terpy = 2,2′:6′,2″-terpyridine).[21] Similar to the oxo-bridged dimanganese catalyst, the thermal decomposition product exhibits good

[*] R. Liu, Y. Lin, S. W. Sheehan, Prof. Dr. D. Wang
Department of Chemistry, Merkert Chemistry Center
Boston College
2609 Beacon St., Chestnut Hill, MA 02467 (USA)
Fax: (+1) 617-552-2705
E-mail: dunwei.wang@bc.edu
Homepage: http://www2.bc.edu/~dwang
L.-Y. Chou, W. He, F. Zhang, Prof. Dr. H. J. M. Hou
Department of Chemistry and Biochemistry
University of Massachusetts Dartmouth
North Dartmouth, MA 02747 (USA)
E-mail: hhou@umassd.edu
Homepage: http://www.faculty.umassd.edu/harveyjianmin.hou/

[**] We acknowledge financial support from Boston College and the University of Massachusetts Dartmouth, technical support from Dr. X. Liu, S. Zhou, Dr. E. Ojadi, C. Leidhold, N. Geh, and S. Cederlund. This work is partially supported by a NSF instrumentation grant (DRM 0821471) to D.W. The XPS experiments were conducted at the Materials Center at MIT.

Supporting information for this article is available on the WWW under http://dx.doi.org/10.1002/anie.201004801.

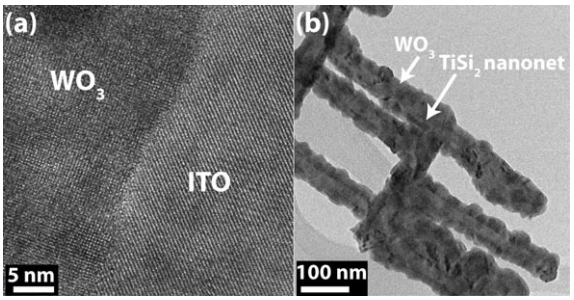

Figure 1. HRTEM images of ALD-grown WO_3. a) Cross-sectional view of WO_3 grown on ITO. The crystalline nature of WO_3 and the atomically sharp interface between WO_3 and ITO demonstrate the advantages of the ALD process. b) WO_3 grown on a $TiSi_2$ nanonet. The uniformity of the WO_3 coating and the conformal coverage show that ALD is a viable approach to prepare heteronanostructures.

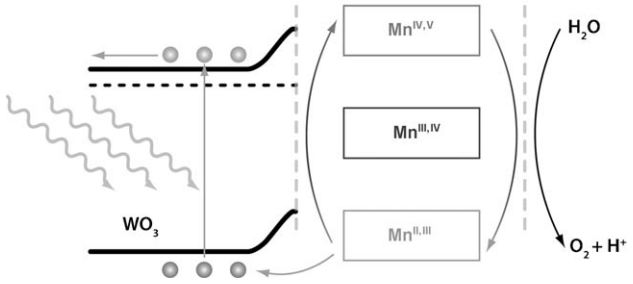

Figure 2. Proposed working mechanism of the WO_3/Mn catalyst system. WO_3 absorbs photons to create electrons and holes, separation of which is assisted by the built-in field within the semiconductor. Electrons are collected, and holes transferred to the catalyst to oxidize H_2O.

catalytic properties when sacrificial oxidants are available.[22] The solid Mn-containing material is not manganese dioxide according to elemental analysis and EPR, FTIR, and atomic absorption spectroscopy.[22] Although further study is needed to understand the exact structure of this catalyst and the nature of its working mechanism, its thermal stability, ease of fabrication, and unequivocal evidence for its catalytic properties compelled us to explore it in the heteronanostructure design.

The surface of WO_3 was coated with the catalyst by thermal treatment of a solution of the above Mn complex at 75 °C (see Experimental Section). This step was brief (typically 5 min) and did not cause noticeable colorization of WO_3. No measurable differences were observed in the absorption spectra of WO_3 before and after this deposition, that is, solvation on the WO_3 surface was insignificant. This observation also suggests that the catalyst poses no appreciable competition to WO_3 in light absorption, which is an extremely important feature, because light absorbed by the catalyst would be wasted. WO_3 can be protected in non-acidic solutions by depositing other materials such as TiO_2 by, for example, ALD. However, deposition of the Mn catalyst is preferred for at least three reasons: 1) deposition is straightforward, 2) the coating does not compete with WO_3 in light absorption, and 3) the catalyst facilitates hole transfer from the semiconductor to the solution (see below).

Figure 2 illustrates the proposed working mechanism of the semiconductor/catalyst system. Light is absorbed by WO_3 to generate electrons and holes. The built-in field in WO_3 helps concentrate electrons away from the solid/liquid interface to be collected by the supporting substrate,[23] which is indium tin oxide (ITO). Holes are driven by the built-in field toward the solid/liquid interface, where they transfer to the solution to oxidize H_2O. This schematic neglects the potential influence of the Mn catalyst coating on the electronic energy of WO_3 because of the thinness of the former. The oxidation process is mediated by the catalyst, which we suggest works in a fashion similar to the oxo-bridged Mn_2 catalyst,[24] that is, mixed-valent Mn^{III} and Mn^{IV} are oxidized by the photogenerated holes from the semiconductor, and the product of the oxidation process is reduced by H_2O to produce O_2. A distinguishing feature of the WO_3/Mn catalyst system is that no sacrificial oxidants are present for O_2 generation. H_2O oxidation by the Mn catalyst is effective and has fast kinetics. When measured in an electrolyte at pH 4, electrodes with and without the Mn catalyst coating exhibited distinct but not significant differences in the photoelectrochemical (PEC) performance (photocurrent and onset potential, see Figure 3a). When the external and internal quantum efficiencies

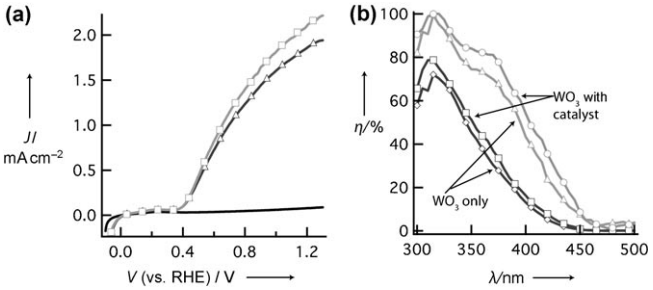

Figure 3. Photoelectrochemical properties of ALD-grown WO_3 and the WO_3/Mn catalyst combination. a) In acidic solutions (pH 4), the presence of the Mn catalyst induces no significant change in the photocurrent (illumination: Hg lamp, 100 mW cm^{-2}) for brief *I–V* scans. □, WO_3 with coating; △, WO_3 only; ——, in the dark. b) This conclusion is supported by measurements of quantum efficiency, η. The differences between the APCE (○ and △) and the IPCE (□ and ◇) also highlight the room for improvement when absorption is improved without impairing charge collection. The heteronanostructure design serves this purpose.

are compared for electrodes with and without the Mn catalyst coating, similar conclusions are reached (Figure 3b). When the catalyst coating is absent, deviation of the photocurrent and the dependence on light intensity from a linear relationship indicates that charge transfer from the semiconductor to the solution becomes a kinetically limiting step.[25] The deviation from linearity is less obvious when the catalyst is present (Figure S6 in the Supporting Information). This suggests that the presence of the catalyst facilitates charge transfer from the semiconductor to the solution, and the effect is more obvious when the charge density is high.

To quantify the amount of O_2 and H_2 generated by the WO_3/Mn catalyst electrode, we conducted photocatalytic experiments with GC analysis. As shown in Figure 4a, a stark

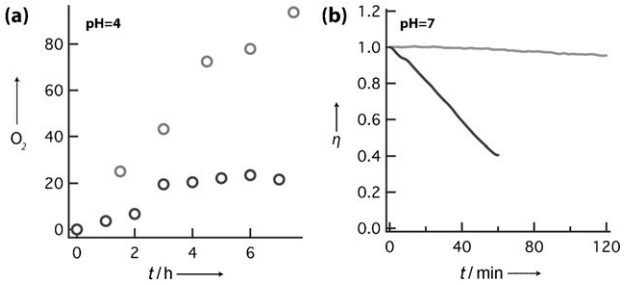

Figure 4. Protecting effect of the Mn catalyst. a) When tested at pH 4, the low rates of oxygen generation [μmol cm^{-2}] by electrodes with (gray ○) and without (black ○) the Mn catalyst are drastically different. This observation contradicts that the photocurrents of these two types of electrodes are comparable and can be attributed to the poor stabilities of WO_3 in high-pH solutions. b) The effect is more pronounced when tested in neutral solutions. After 2 h, the performance of the electrode with the Mn catalyst (gray line) decreases by approximately 4%, whereas that without the catalyst (black line) drops by 60% within 1 h.

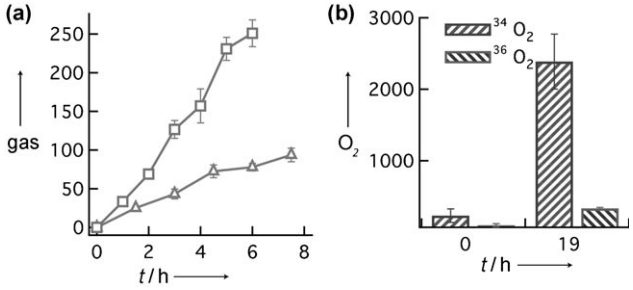

Figure 5. Photocatalytic experiments confirm that the measured O_2 is the direct product of complete H_2O splitting. a) The rate of H_2 production [μmol cm^{-2}] (□) is approximately twice that of O_2 (△). b) Isotopic labeling experiments (arbitary units) verify that oxygen atoms in O_2 come from H_2O.

difference is observed for the electrodes with and without the Mn catalyst. When the catalyst is present, the amount of O_2 increases with time, following a linear relationship for up to 5 h, after which the rate of O_2 generation slows down. The reduced rate of O_2 generation is caused by the experimental design. When the vessel was purged with N_2 and the experiment was restarted, O_2 was produced at the same rate as in the original experiment (see Supporting Information). Without the Mn catalyst, the amount of O_2 measured was only approximately 50% of that with the Mn catalyst after 3 h. Thereafter, the electrode ceased to function, showed obvious colorization, and eventually peeled off from the ITO support. Better stability was observed when solutions with lower pH were used, and no obvious colorization was seen when WO_3 was tested in solutions of pH 2 for up to a day. The protecting effect of the Mn catalyst was more pronounced when the electrodes were tested in less acidic solutions. At pH 7, WO_3 without the Mn catalyst decayed more quickly than at pH 4 (60% after 1 h), whereas approximately 4% performance degradation was observed when the Mn catalyst was present (Figure 4b) for up to 2 h. It took more than 19 h in the Mn/WO_3 case for the efficiency to drop to 50% of the initial value.

Various evidence supports that the detected O_2 is the direct product of H_2O splitting. First, the amount of H_2 is approximately twice that of O_2, consistent with complete decomposition of H_2O (Figure 5a). Second, control experiments with $H_2{}^{18}O$ confirmed that O in the gas phase comes from H_2O (Figure 5b).[26] Third, the amount of O_2 far exceeds what would be available in WO_3 or the Mn catalyst. The rate of O_2 generation was measured by GC to be 13.6 μmol cm^{-2} h^{-1}. The rate was also calculated from the measured photocurrent as 16.8 μmol cm^{-2} h^{-1} (based on a current density of 1.8 mA cm^{-2}). The discrepancy originates from the GC measurements, which did not include O_2 dissolved in the solution or lost due to imperfections of the apparatus. Improvement of the GC method by, for example, using a flow-through system will correct this. Using literature methods, we computed a peak energy-conversion efficiency of 1.1% (at 0.80 V vs. reversible hydrogen electrode (RHE)), and the efficiency was 0.59% at $V = 1.23$ V (vs. RHE, see Supporting Information). Although the observed photocurrent at 1.23 V (vs. RHE) is among the highest for WO_3, the efficiency is still low compared with solar cells. Weak absorption in the visible range is the primary reason for the low efficiency (Figure 3b). Nonetheless, the stability of the resulting material in neutral solutions is significant and has not been reported previously.

Efficiently and inexpensively converting solar energy by splitting H_2O is one of the most pressing issues we face today. Research in this area faces a multitude of challenges. Capabilities to design, make, and study novel materials that can perform this reaction with meaningful efficiency and at low cost have broad appeal. The results presented here will contribute significantly to this goal. The ALD growth of WO_3 without production of corrosive byproducts has not been reported elsewhere, and the synthetic technique makes it easy to form heteronanostructures. The Mn catalyst derived from the oxo-bridged Mn dimer is easy to prepare and exhibits good stability and catalytic properties. When interfaced with WO_3, it acts as a protecting layer without adverse effect on the water-splitting properties. To the best of our knowledge, this is the first time that WO_3 photoelectrodes stable in neutral solution have been prepared. The heteronanostructure design combines multiple components, each with unique complementary and critical functions, and offers combinations of properties that are not available in single-component materials. The versatility of this method will find applications in numerous areas where the availability of materials is the limiting factor.

Experimental Section

ALD growth of WO_3: WO_3 was synthesized in a Savannah 100 ALD system (Cambridge Nanotech) from (tBuN)$_2$(Me$_2$N)$_2$W (97%, Aldrich), which was heated at 75 °C, and deionized H_2O, which was kept at room temperature, as precursors for tungsten and oxygen, respectively. The substrate, an ITO-coated glass substrate (Nanocs, 10 Ω sq^{-1}), was heated to temperatures between 250 and 350 °C. A constant N_2 flow of 10 standard cubic centimeters per minute (sccm) served as the purge gas. A growth rate of 1.0 Å per cycle was achieved. After synthesis, the resulting WO_3 film was annealed in a tube furnace at 550 °C with 100 sccm O_2 flow at atmosphere pressure. The annealing process lasted 1 h.

Preparation of the Mn catalyst: The Mn catalyst was prepared by following published protocols.[21] In a typical experiment, $Mn(OAc)_2$ (1.06 g, 4.29 mmol) and 2,2′:6,2″-terpyridine (1.00 g, 4.29 mmol) were dissolved in 15 mL of H_2O, and then $KHSO_5$ (1.04 g, 3.21 mmol) in 15 mL of water was added dropwise with stirring, which turned the yellow solution dark green. After stirring at room temperature for 10 min, the solution was cooled to 0 °C. 20 mL of saturated KNO_3 solution was then added, resulting in a green precipitate of the oxo-bridged Mn dimer (2.31 g, 65.0 %). Elemental analysis revealed a formula of $C_{30}H_{26}N_9O_{13}Mn_2$. More details of the elemental analysis are available in the Supporting Information. At room temperature, the Mn complex was redissolved in H_2O to make a 1 mM solution. When heated to 75 °C, the oxo-bridged Mn dimer underwent thermal decomposition to yield the Mn catalyst, which was received by the WO_3 film. The thickness of the catalyst coating was controlled by varying the concentration of the Mn complex. The deposition time was kept constant at 5 min. More details of controlling deposition thickness are available in the Supporting Information.

Photoelectrochemical (PEC) experiments: The resulting WO_3 (thickness: 180 nm) with or without the Mn catalyst was fabricated into a working electrode in a fashion similar to our previous report.[8] A Pt mesh was used as counterelectrode, and the reference electrode was Ag/AgCl in 1M KCl solution. The electrolyte solution was 1M KCl with HCl added to adjust the pH from 2 to 7. A CHI 600C potentiostat was used. The voltage was swept between 0 and 1.3 V (vs. RHE) at a rate of 10 $mV\,s^{-1}$. The light source was a 150 W Newport Mercury lamp, and the intensity was adjusted to 100 $mW\,cm^{-2}$. The incident-photon-to-charge conversion efficiency (IPCE) and the absorbed-photon-to-charge conversion efficiency (APCE) were measured by using a Newport quantum efficiency measurement kit (QE-PV-SI). For the IPCE and the APCE experiments, the working electrode was biased at 1.23 V (vs. RHE). The absorption spectra were collected with an Ocean Optics spectrometer (USB 4000) and an integration sphere (Sphere Optics, RT-4Z).

GC analysis: To quantify the amount of oxygen and hydrogen generated by the water splitting process, the PEC apparatus was sealed in an N_2 environment. The working electrode bias was fixed at 1.23 V (vs. RHE). The gas phase was sampled periodically, and the samples were fed to an HP 5890 gas chromatograph equipped with an HP-PLOT MoleSeive column. The temperatures of the injector and the detector were set at 100 °C. Helium and nitrogen were used as carrier gases for oxygen and hydrogen, respectively. For the GC-MS analysis, a Thermo Fisher Scientific ITQ 700 with a Focus GC was utilized. Detailed parameters for these experiments are available in the Supporting Information.

Structural characterization: A transmission electron microscope (TEM, JEM-2010F, operating at 200 keV) was used to study cross-section samples of ALD-grown WO_3, prepared by using a focused ion beam (FIB, JOEL 4500 Multibeam system). More details of the sample preparation are available in the Supporting Information.

Received: August 2, 2010
Published online: December 9, 2010

Keywords: electrochemistry · nanostructures · photochemistry · solar energy · water splitting

[1] J. R. Bolton, *Solar Energy* **1996**, *57*, 37 – 50.
[2] A. Fujishima, K. Honda, *Nature* **1972**, *238*, 37 – 38.
[3] D. G. Nocera, *Chem. Soc. Rev.* **2009**, *38*, 13 – 15.
[4] N. S. Lewis, D. G. Nocera, *Proc. Natl. Acad. Sci. USA* **2006**, *103*, 15729 – 15735.
[5] T. Bak, J. Nowotny, M. Rekas, C. C. Sorrell, *Int. J. Hydrogen Energy* **2002**, *27*, 991 – 1022.
[6] M. Woodhouse, B. A. Parkinson, *Chem. Soc. Rev.* **2009**, *38*, 197 – 210.
[7] M. Dare-Edwards, J. Goodenough, A. Hamnett, P. Trevellick, *J. Chem. Soc. Faraday Trans. 1* **1983**, *79*, 2027 – 2041.
[8] Y. Lin, S. Zhou, X. Liu, S. Sheehan, D. Wang, *J. Am. Chem. Soc.* **2009**, *131*, 2772 – 2773.
[9] S. Zhou, X. H. Liu, D. W. Wang, *Nano Lett.* **2010**, *10*, 860 – 863.
[10] D. K. Zhong, J. Sun, H. Inumaru, D. R. Gamelin, *J. Am. Chem. Soc.* **2009**, *131*, 6086 – 6087.
[11] W. J. Youngblood, S.-H. A. Lee, Y. Kobayashi, E. A. Hernandez-Pagan, P. G. Hoertz, T. A. Moore, A. L. Moore, D. Gust, T. E. Mallouk, *J. Am. Chem. Soc.* **2009**, *131*, 926 – 927.
[12] S. D. Tilley, M. Cornuz, K. Sivula, M. Grätzel, *Angew. Chem.* **2010**, *122*, 6549 – 6552; *Angew. Chem. Int. Ed.* **2010**, *49*, 6405 – 6408.
[13] M. Butler, *J. Appl. Phys.* **1977**, *48*, 1914 – 1920.
[14] C. Santato, M. Odziemkowski, M. Ulmann, J. Augustynski, *J. Am. Chem. Soc.* **2001**, *123*, 10639 – 10649.
[15] A. Kudo, *Int. J. Hydrogen Energy* **2007**, *32*, 2673 – 2678.
[16] P. Tagtstrom, P. Martensson, U. Jansson, J. O. Carlsson, *J. Electrochem. Soc.* **1999**, *146*, 3139 – 3143.
[17] G. A. Niklasson, C. G. Granqvist, *J. Mater. Chem.* **2007**, *17*, 127 – 156.
[18] S. Zhou, X. H. Liu, Y. J. Lin, D. W. Wang, *Angew. Chem.* **2008**, *120*, 7795 – 7798; *Angew. Chem. Int. Ed.* **2008**, *47*, 7681 – 7684.
[19] S. Zhou, X. Liu, Y. Lin, D. Wang, *Chem. Mater.* **2009**, *21*, 1023 – 1027.
[20] R. S. Lillard, G. S. Kanner, D. P. Butt, *J. Electrochem. Soc.* **1998**, *145*, 2718 – 2725.
[21] J. Limburg, J. S. Vrettos, L. M. Liable-Sands, A. L. Rheingold, R. H. Crabtree, G. W. Brudvig, *Science* **1999**, *283*, 1524 – 1527.
[22] F. Zhang, C. Cady, G. W. Brudvig, H. J. M. Hou, *Inorg. Chim. Acta* **2010**, DOI: 10.1016/j.ica.2010.10.021.
[23] M. Grätzel, *Nature* **2001**, *414*, 338 – 344.
[24] G. W. Brudvig, *Philos. Trans. R. Soc. London Ser. B* **2008**, *363*, 1211 – 1219.
[25] T. Lindgren, H. Wang, N. Beermann, L. Vayssieres, A. Hagfeldt, S.-E. Lindquist, *Sol. Energy Mater. Sol. Cells* **2002**, *71*, 231 – 243.
[26] M. Kanan, D. G. Nocera, *Science* **2008**, *321*, 1072 – 1075.

